ENDOR and Special Triple Resonance Spectroscopy of $A_1^{\bullet-}$ of Photosystem 1[†]

Stephen E. J. Rigby,[‡,§] Michael C. W. Evans,[‡] and Peter Heathcote*[,||]

Department of Biology, Darwin Building, University College London, University of London, London WC1E 6BT, U.K., and School of Biological Sciences, Queen Mary and Westfield College, University of London, Mile End Road, London E1 4NS, U.K.

Received November 3, 1995; Revised Manuscript Received March 11, 1996[⊗]

ABSTRACT: The photoaccumulated radical state of the photosystem 1 secondary electron acceptor A_1, $A_1^{\bullet-}$, has been studied in spinach and the cyanobacterium *Anabaena variabilis* strain Met27 using electron nuclear double resonance (ENDOR) and electron−nuclear−nuclear special triple (ST) resonance spectroscopies. Spectra of $A_1^{\bullet-}$ in both these species are very similar. ENDOR spectra of the phylloquinone anion radical in solvent glass were also obtained. Comparison of the spectra of the *in vivo* and *in vitro* radicals shows that $A_1^{\bullet-}$ is a phylloquinone anion radical with a distorted electron spin density distribution. Hyperfine couplings to the $A_1^{\bullet-}$ methyl group and to two protons hydrogen bonded to the quinone oxygens have been identified using biosynthetic deuteration in *A. variabilis*. Possible hyperfine coupling to a methylene proton of the phytyl side chain of the quinone has also been identified. These results are compared with those from previous studies of protein-bound semiquinones in the light of the unusual redox potential of A_1.

Quinones function as both mobile and protein bound redox cofactors in many biological processes including respiration and photosynthesis. The association of quinones with proteins allows for the modification of the properties of the quinone by its protein environment. This is illustrated by the best characterized quinone binding protein, the photosynthetic reaction center of the purple bacterium *Rhodobacter sphaeroides* (see Deisenhofer and Norris (1993) for a review). Here, two molecules of ubiquinone are bound to the protein; one, Q_A, is an electron carrier which cannot be protonated, whereas the other, Q_B, is protonated in its two electron reduced state and has a more positive E_m than Q_A, by which it is reduced.

Quinones are also found in photosystem 1 (PS1)[1] of oxygenic photosynthesis. The electron transfer pathway of green plant and cyanobacterial PS1 (Golbeck, 1992; Evans & Nugent, 1993) starts with the photooxidation of a chlorophyll *a* pair (P700), the expelled electron reducing another chlorophyll *a* molecule designated A_0. From here the electron passes to a further acceptor A_1, and from here to an iron sulfur center chain consisting of centers Fe-S_X, Fe-S_A, and Fe-S_B, respectively. Several lines of evidence indicate that the secondary electron acceptor A_1 is phylloquinone (Evans & Nugent, 1993). Extraction of phylloquinone from PS1 abolishes the photoaccumulated EPR spectrum attributed to $A_1^{\bullet-}$ (Itoh et al., 1987; Mansfield et al., 1987) and the electron spin polarized (ESP) signal arising from the $P700^{+\bullet}-A_1^{\bullet-}$ radical pair (Rustandi et al., 1990). The ESP signal is also affected when PS1 is reconstituted with deuterated phylloquinone (Rustandi et al., 1990). Additionally, extraction of phylloquinone abolishes forward electron transfer at room temperature (Biggins & Mathis, 1988). Further recent evidence has shown that A_1 may be double reduced at pH 10 (Setif & Bottin, 1989, 1991; Heathcote et al., 1993). This is a property of quinones and not of chlorophylls or amino acid residues. Double reduction abolishes the photoaccumulated EPR spectrum (Heathcote et al., 1993) and the ESP signal mentioned above (Snyder et al., 1991). Contrary evidence has nevertheless been forthcoming from UV photodestruction experiments (Palace et al., 1987; Ziegler et al., 1987) and a study in which the effect of incorporating deuterium label into quinones on the photoaccumulated EPR spectrum was examined (Barry et al., 1988). However, there is conflicting evidence as to whether UV photodestruction abolishes forward electron transfer. Heathcote et al. (1996) have shown that incorporating deuterium biosynthetically into phylloquinone does narrow the photoaccumulated EPR spectrum; these experiments may be in disagreement with the earlier (Barry et al., 1988) work because the possibility of double reduction had not been considered at that time.

In order to transfer electrons from A_0 to Fe-S_X, A_1 must have an E_m of *ca.* −800 mV (Evans & Nugent, 1993); however, phylloquinone has an E_m of only *ca.* −100 mV *in vitro*. Therefore, interaction with the protein lowers the E_m of the bound phylloquinone by 700 mV relative to *in vitro*. This suggests that the protein is effecting a large change in the electronic structure of the bound quinone.

$A_1^{\bullet-}$ can be photoaccumulated by brief illumination at 205 K in the presence of dithionite (Mansfield & Evans, 1988; Heathcote et al., 1993, 1996). This allows for the formation of the $A_1^{\bullet-}$ EPR signal which in turn opens up the possibility of using electron nuclear double resonance (ENDOR) spectroscopy (Dorio & Freed, 1979; Kurreck et al., 1988). ENDOR spectroscopy reveals the electronic structures of

[†] We acknowledge financial support from the U.K. Biotechnology and Biological Sciences Research Council (BBSRC).

* Corresponding author.
[‡] University College London.
[§] Present address: School of Biological Sciences, Queen Mary and Westfield College.
[||] Queen Mary and Westfield College.

[⊗] Abstract published in *Advance ACS Abstracts,* May 1, 1996.

[1] Abbreviations: A_1, phylloquinone secondary electron acceptor of photosystem 1; ENDOR, electron nuclear double resonance spectroscopy; EPR, electron paramagnetic resonance spectroscopy; hfc, hyperfine coupling constant; PS1, photosystem 1; ν_H, proton Larmor frequency; SOMO, singly occupied molecular orbital; ST, special triple resonance spectroscopy.

S0006-2960(95)02619-5 CCC: $12.00

radicals, as expressed in the unpaired electron spin density distribution of the singly occupied molecular orbital (SOMO). Here we report the first study of $A_1^{\bullet-}$ in PS1 from spinach and the cyanobacterium *Anabaena variabilis*, together with the phylloquinone anion radical ($PhQ^{\bullet-}$) *in vitro*, using ENDOR and the related technique of electron−nuclear−nuclear special triple resonance (ST) (Freed, 1969; Dinse et al., 1974) spectroscopies. The availability of a methionine auxotrophic strain (Met27) of the cyanobacterium *A. variabilis* (Currier et al., 1977) enabled us to use *in vivo* deuteration of the quinone as a spectrum assignment tool. The results demonstrate the effects of the protein on the electronic structure of A_1, which may account for its unusual E_m.

MATERIALS AND METHODS

Growth of the cyanobacterium *A. variabilis* Met27, and preparation of photosystem I particles from these cells and from spinach, is as described in Heathcote et al. (1996). The phylloquinone anion radical $A_1^{\bullet-}$ was photoaccumulated in photosystem 1 by 205 K illumination in the presence of dithionite as described in Heathcote et al. (1993, 1996). The phylloquinone and 2-methylnaphthoquinone anion radicals were produced by stoichiometric sodium borohydride reduction of alkaline ethanolic solutions of the appropriate quinone under a stream of argon (Hales & Case, 1981). The radical solutions were then rapidly frozen in liquid nitrogen.

ENDOR, ST, and EPR spectra were obtained at X-band using a Bruker ESP 300 EPR spectrometer as described in Rigby et al. (1994a,b). Spectra were corrected for a small baseline nonlinearity by the subtraction of off-resonance scans which were filtered for noise (standard Bruker software) to avoid reducing the spectrum signal to noise ratio. The experimental spectra were not filtered for noise. Acquisition conditions for specific spectra are given in the figure captions. Characteristic ENDOR and ST lineshapes were established by examining several sets of samples involving different PS1 preparations. Precision of hfc determination, i.e., the variation in hfc determination between these samples, was ±0.1 MHz. Spectra are presented in first derivative mode. The hyperfine coupling constants are measured from zero crossing points, except for $A_{||}$ features, where the peak maximum/minimum is used.

RESULTS

Figure 1a shows the EPR spectrum in the $g = 2.00$ region produced by illuminating *A. variabilis* Met27 (grown on protonated methionine) PS1 particles for 2 min at 205 K in the presence of sodium dithionite (Heathcote et al., 1993). The spectrum, with $g = 2.0048$ and ΔH_{ptp} of 0.95 mT, is essentially identical to that reported for spinach digitonin PS1 particles by Heathcote et al. (1993) and assigned to the reduced form of A_1, $A_1^{\bullet-}$. Figure 1d shows the EPR spectrum of the phylloquinone anion radical, $PhQ^{\bullet-}$, freeze trapped in an alkaline ethanol glass. While the g and ΔH_{ptp} values of the two signals are the same, the EPR spectrum of $A_1^{\bullet-}$ is noticeably less symmetrical than that of $PhQ^{\bullet-}$. Particularly evident is a shoulder at the low-field, g_x, side of the $A_1^{\bullet-}$ spectrum which is absent in the spectrum of $PhQ^{\bullet-}$.

The ENDOR spectrum of protonated *A. variabilis* $A_1^{\bullet-}$ is presented in Figure 2a. This region of the ENDOR spectrum shows features arising from hyperfine coupling to proton (hydrogen) nuclei. Frozen solution ENDOR spectra of radicals taken at the EPR crossing point typically show all orientations of the molecules in the external field simultaneously (i.e., a powder spectrum). Therefore, the lineshapes observed reflect the symmetry of the hyperfine tensors and the random orientation of the tensors in the applied field. Features 2 and 4 of Figure 2a are particularly prominent, while features 1 and 3 are much less intense. The most intense features of frozen solution quinone radical ENDOR spectra arise from the A_1 components of the axially symmetric hfcs to protons hydrogen bonded to the quinone

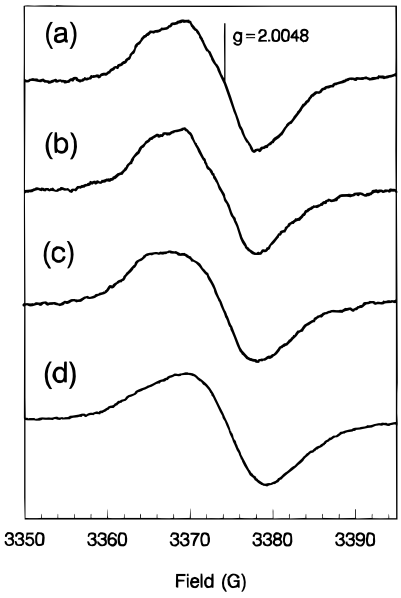

FIGURE 1: EPR spectra of $A_1^{\bullet-}$ in (a) *A. variabilis* membranes, (b) spinach digitonin particles, and (c) spinach Triton X-100 particles, all produced by 2 min illumination at 205 K in the presence of dithionite. (d) EPR spectrum of the phylloquinone anion radical $PhQ^{\bullet-}$ in alkaline ethanol produced by borohydride reduction under argon. Experimental conditions: microwave power, 40 μW; modulation amplitude, 1.2 G; modulation frequency, 12.5 kHz; temperature, 60 K; (a)−(c) are the sums of four scans; all spectra recorded in the ENDOR cavity.

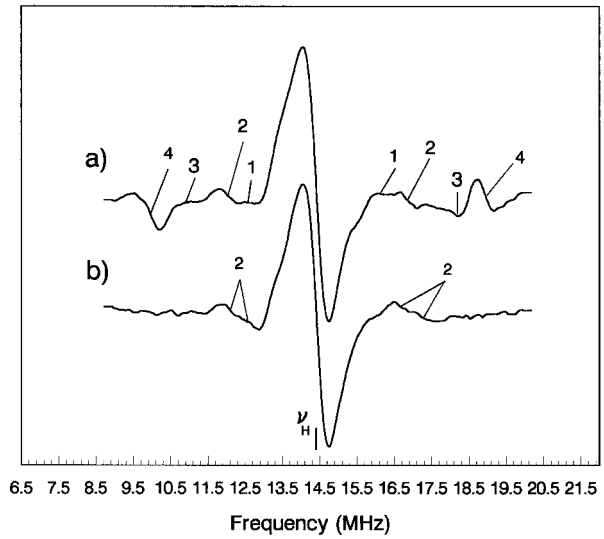

FIGURE 2: ENDOR spectra of $A_1^{\bullet-}$ in *A. variabilis* grown on (a) protonated and (b) [*methyl*-d_3]methionine at 60 K. Numbers refer to features assigned in Table 1. Experimental conditions: microwave power, 7.9 mW; rf power, 100 W; rf modulation depth, 200 kHz; scan time, 84 s; time constant, 1310 ms; sum of 200 scans.

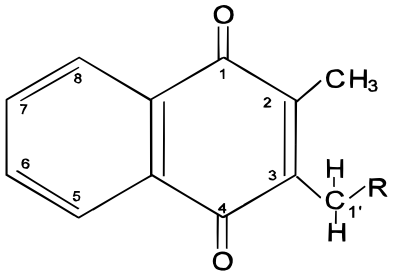

FIGURE 3: Structure of phylloquinone with carbon atom numbering scheme. R is $CHCCH_3CH_2(CH_2CH_2CHCH_3CH_2)_3H$.

oxygens (O'Malley & Babcock, 1986) and the protons of methyl groups β to the delocalized π orbital system (O'Malley & Babcock, 1984) bearing the unpaired electron [i.e., the singly occupied molecular orbital (SOMO)]. Both methyl group and hydrogen bond hfcs have been shown to possess axial lineshapes in frozen solution ENDOR, each having an intense $A_\perp$ component which shows a zero crossing and a weaker $A_\parallel$ turning point (O'Malley & Babcock, 1984, 1986). Hfcs to methylene protons β to the SOMO may also be observed under some circumstances as in ENDOR studies of tyrosine radicals (Hoganson & Babcock, 1992; Rigby et al., 1994a).

To distinguish between methyl and hydrogen bonded protons, we have taken advantage of the methionine growth requirement (auxotrophy) of our *A. variabilis* strain Met27 to introduce deuterium label into A_1. Growth on [*methyl*-d_3]methionine should deuterate only the quinone methyl group at C(2) (Barry & Babcock, 1987; see Figure 3 for phylloquinone structure and numbering scheme). However, our results suggest more extensive labeling of the phylloquinone (see Heathcote et al., 1996), with deuterium being incorporated in the phytyl side chain at C(3) as well as the C(2) methyl group. This is the same isotope labeling experiment used in Barry et al. (1988), but the conditions for the photoaccumulation of $A_1^{\bullet-}$ are very different here (see Materials and Methods and discussed in Heathcote et al., 1996). The ENDOR spectrum of $A_1^{\bullet-}$ obtained from *A. variabilis* grown on [*methyl*-d_3]methionine is shown in Figure 2b. The lineshape of feature 4, together with its absence from Figure 2b, suggests that this feature arises from the $A_\perp$ component of the 2-methyl group hfc. Feature 2 is assigned as the $A_\perp$ component of a hydrogen bond hfc from its insensitivity to deuteration. The nature (proton or deuteron) of the hydrogen bonded "protons" is determined by the solvent (H_2O or D_2O) in which the cyanobacteria were grown and in which the PS1 was purified, not by the incorporation of deuterated methionine. Since the cyanobacteria were grown and the PS1 purified in H_2O, the H-bond resonances would be expected to be the same in both Figures 2a and 2b. Two hydrogen bonds (one to each oxygen) might be expected for phylloquinone, and therefore feature 2 may arise from the degenerate hfcs to both oxygens of the quinone. Indeed, in Figure 2b feature 2 seems to show partial resolution into two features, suggesting the degeneracy is not complete. The attenuation of the weak features 1 and 3 in Figure 2b confirms that the deuterium label is not confined to the 2-methyl group and that some deuteration of other protons on the quinone occurs. Features 1 and 3 can therefore be assigned as hfcs to a quinone proton, probably one of the 1′-methylene protons attached to C(3). The hfcs of features 1−4 are collected in Table 1. A previous

Table 1: Hyperfine Coupling Constants and Resonance Assignments for $A_1^{\bullet-}$ and for the Phylloquinone Anion Radical ($PhQ^{\bullet-}$) in Alkaline Ethanol

	hyperfine coupling constant (MHz)[a]			
	$A_1^{\bullet-}$			
feature	*A. variabilis*	spinach	$PhQ^{\bullet-}$	assignment
1	3.6	3.6	3.0	?3-β-CH_2 $A_\perp$
2	−5.0[b]	−5.2[b]	−2.2[b]	H-bond $A_\perp$
	−5.8[b]	−6.0[b]		H-bond $A_\perp$
3	7.6	7.7	−[c]	?3-β-CH_2 $A_\parallel$
4	9.0	9.0	6.8	2-methyl $A_\perp$
5	12.8	12.6	10.0	2-methyl $A_\parallel$[d]
	(10.3	10.2	7.9	2-methyl A_{iso})
	13.4	13.4		H-bond $A_\parallel$[d]
*			5.2	H-bond $A_\parallel$[e]

[a] Accuracy of hfc measurement estimated at ±0.1 MHz. [b] The attribution of negative signs to the perpendicular components of hydrogen bond couplings follows from Muto and Iwasaki (1973) and O'Malley and Babcock (1986). [c] This feature was not detected for $PhQ^{\bullet-}$. [d] The constituent components of feature 5 cannot be assigned definitively, but this assignment is consistent with the known properties of quinone methyl and H-bond hfcs. [e] This is the resonance labeled * on Figure 5.

ENDOR study of the phylloquinone anion radical in ethanolic liquid solution (Barry et al., 1988) has shown that the hfcs to the aromatic protons at carbons 5−8 are small, *ca*. 2 MHz or less, and are thus hidden under the central "matrix" feature in frozen solution studies.

The resolution of features 1 and 2 of Figure 2 could be improved by recording the spectrum using lower rf modulation depth. However, this would carry an unacceptable signal to noise penalty. Therefore, we have used the increase in the signal to noise ratio prioduced by electron−nuclear−nuclear special triple resonance (ST) spectroscopy (Freed, 1969; Dinse et al., 1974) to offset the signal to noise losses at lower modulation depths. ST spectroscopy produces a "half ENDOR" spectrum with increased intensity, in which the hfcs can be read off as twice the frequency axis position. The ST spectrum of $A_1^{\bullet-}$ in *A. variabilis* (without deuteration) acquired with an rf modulation depth of 158 kHz is shown in Figure 4a. Feature 1 is well resolved in this spectrum, and its first derivative lineshape suggests it arises from the $A_\perp$ component of an hfc to a 1′-methylene proton attached at C(3). Feature 2 is clearly split into two components, confirming H-bonding to both oxygens in $A_1^{\bullet-}$. Feature 3 appears in this spectrum as a shallow depression, possibly arising from the $A_\parallel$ feature of the hfc to a 1′-methylene proton at C(3). The ST technique has also revealed a new feature (labeled 5, see Table 1) which we assign as the overlapped $A_\parallel$ components of the H-bond and methyl couplings. H-bond hfcs are expected to be approximately traceless, i.e., $A_\parallel + 2A_\perp = -0.03$ to $+1.37$ (Lubitz et al., 1985; O'Malley & Babcock, 1986; MacMillan et al., 1995; Rigby et al., 1995), with the small isotropic component of the hfc arising from unpaired spin transferred to the hydrogen bonded proton, while $A_\parallel - A_\perp = 3-3.5$ MHz for quinone methyl groups (O'Malley & Babcock, 1984). Therefore, the lineshape and hfc(s) assigned to feature 5 fulfill the criteria for assignment as $A_\parallel$ components of both methyl and H-bond hfcs for which the $A_\perp$ components were identified above. While the multicomponent nature of feature 5 is evident from its intensity and the observation of at least two minima, it is not possible to associate particular

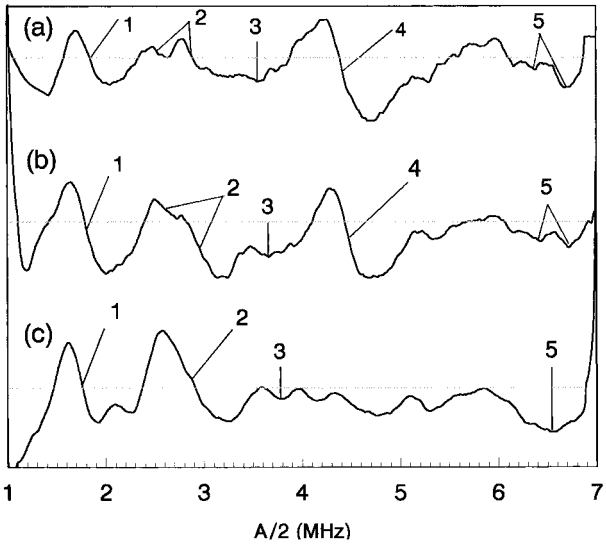

FIGURE 4: Electron−nuclear−nuclear special triple spectra of $A_1^{\bullet-}$ in (a) *A. variabilis* membranes, (b) spinach digitonin particles, and (c) spinach Triton X-100 particles at 60 K. Numbers refer to features assigned in Table 1. Experimental conditions: microwave power, 10 mW; rf power, 200 W (total over both channels); rf modulation depth, 158 kHz; scan time, 84 s; time constant, 655 ms; (a) and (c) sums of 240 scans, (b) sum of 300 scans.

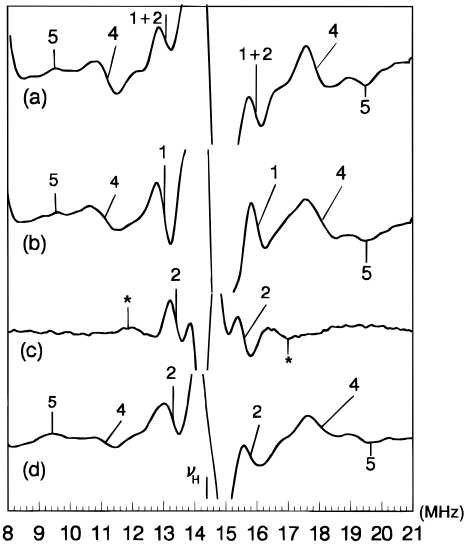

FIGURE 5: ENDOR spectra of model naphthoquinone anion radicals at 60 K. (a) Phylloquinone anion radical ($PhQ^{\bullet-}$) in alkaline ethanol; (b) phylloquinone anion radical ($PhQ^{\bullet-}$) in alkaline ethanol-d (i.e., deuterated); (c) difference (a) minus (b) showing features arising from an hfc to hydrogen bonded protons; * marks a feature only visible in the difference spectrum; (d) 2-methylnaphthoquinone anion radical ($2MNQ^{\bullet-}$) in alkaline ethanol. Numbers refer to features assigned in Table 1. Experimental conditions: microwave power, 7.9 mW; rf power, 100 W; rf modulation depth, 100 kHz; scan time, 84 s; time constant, 655 ms; sums of 40 scans.

minima, and hence $A_{||}$ components, with their corresponding $A_\perp$ features.

The EPR spectra of $A_1^{\bullet-}$ produced in spinach digitonin and Triton X-100 preparations by 205 K in the presence of dithionite are shown as Figures 1b and 1c, respectively. They agree well with those previously reported for these species (Mansfield & Evans, 1988; Heathcote et al., 1993). The EPR spectrum of the radical formed in the digitonin preparation shows the same apparent increase in g_x relative to $PhQ^{\bullet-}$ *in vitro* as the *A. variabilis* spectrum, Figure 1a. The EPR spectrum from the Triton preparation, however, appears broader but more isotropic than the *A. variabilis* spectrum. Using the signal to noise advantage of ST spectra discussed above, hfcs for $A_1^{\bullet-}$ in spinach digitonin particles (Figure 4b) and Triton X-100 particles (Figure 4c) have also been obtained. Figure 4b shows essentially the same features as Figure 4a, suggesting that the electronic structure and H-bonding of $A_1^{\bullet-}$ in spinach digitonin particles and *A. variabilis* are very similar. The ST spectrum of $A_1^{\bullet-}$ in the spinach Triton X-100 preparation (Figure 4c) is, however, rather different. The resolution of the H-bond $A_\perp$ feature (feature 2) into two components is reduced, and several weak features appear in place of the strong 2-methyl $A_\perp$ components (feature 4) of Figures 4a and 4b. This suggests isolation and purification of PS1 using Triton X-100 affects the environment and electronic structure of A_1, leading to heterogeneity in the spin density at C(2) and possibly the loss or alteration of one H-bond hfc. Hfcs for $A_1^{\bullet-}$ in both spinach preparations are collected in Table 1.

The 2-methyl group hfc measured for $A_1^{\bullet-}$ is larger than that previously determined for the phylloquinone anion radical ($PhQ^{\bullet-}$) in liquid ethanolic solution (Barry et al., 1988). Therefore, to provide for a more suitable comparison, we have measured ENDOR spectra of $PhQ^{\bullet-}$ in frozen alkaline ethanol glasses (Figure 5). The feature numbering scheme used in the $A_1^{\bullet-}$ studies above has been maintained to aid comparison. The spectrum, Figure 5a, shows two major first derivative features, labeled 1+2 and 4, and a turning point, feature 5. Comparison of these properties with previous ENDOR studies of quinone anion radicals in frozen solutions (O'Malley & Babcock, 1984, 1986) assigns features 4 and 5 as the $A_\perp$ and $A_{||}$ components, respectively, of the hfc to the 2-methyl group. Feature 1+2 might be expected to be the $A_\perp$ component of the hfc to a hydrogen-bonded proton. This assertion can be tested by recording the spectrum of $PhQ^{\bullet-}$ in deuterated solvent, Figure 5b. Features 4 and 5 are unaffected by solvent deuteration, consistent with their assignment as 2-methyl hfc components. However, the lineshape of feature 1+2 is altered, and the hfc associated with this resonance is increased slightly from 2.8 to 3.0 MHz. Taking the difference between Figures 5a and 5b reveals an underlying spectrum, Figure 5c, which consists of one first derivative feature and one turning point. These features arise from the $A_\perp$ and $A_{||}$ components, respectively, of the hfc to an exchangeable, hydrogen-bonded proton which is replaced by a deuteron in the species of Figure 5b. Feature 1+2 of Figure 5a is therefore a composite of the hydrogen bond $A_\perp$ (labeled feature 2) and the deuteration insensitive feature 1 of Figure 5b. Feature 1 might be a component of the hfc to the 1′-methylene group of the phytyl side chain. Where the phytyl side chain is replaced by a single hydrogen atom to produce 2-methylnaphthoquinone, the ENDOR spectrum of the anion radical, Figure 5d, shows hfcs to the methyl group, features 4 and 5, and to the hydrogen bonded proton, feature 2, but there is no equivalent of feature 1 confirming its assignment to a 1′-methylene proton hfc. Hfcs for $PhQ^{\bullet-}$ are given in Table 1.

DISCUSSION

The data collected in Table 1 reveal large differences between the hfcs of $A_1^{\bullet-}$ and $PhQ^{\bullet-}$. These differences are much larger than those reported for the binding of ubiquinone

to the Q_A site of the *R. sphaeroides* photosynthetic reaction center (Lubitz et al., 1985) or plastoquinone to the Q_A site of photosystem 2 (MacMillan et al., 1995; Rigby et al., 1995). The *R. sphaeroides* system shows a decrease in the 3-methyl (IUPAC numbering; this group is at the equivalent structural position of the 2-methyl in phylloquinone and is labeled the 5-methyl of ubiquinone in Lubitz et al., 1985) group A_{iso} from 5.7 to 5.0 MHz on binding to the reaction center, whereas the A_{iso} of the 2-methyl group of phylloquinone increases from 7.9 to 10.3 MHz when bound at the A_1 site of PS1. This presumably reflects the very different properties conferred on the quinones through binding to their respective proteins. However, despite these large differences in the hfcs, the ENDOR and ST spectra of $A_1^{\bullet-}$ are still consistent with it being a phylloquinone anion radical. For both $A_1^{\bullet-}$ and $PhQ^{\bullet-}$, the largest hfc attributed to a covalently attached proton is to a methyl group with $A_{||} - A_{\perp}$ of *ca*. 3.5 MHz, which is typical of quinone methyl groups. It is difficult to conceive of how any chlorophyll or aromatic amino acid reporter molecule radical (Barry et al., 1988) could give rise to such an hfc and to the two large H-bond hfcs observed.

The hfcs of β methyl groups are related to the unpaired electron spin density at the attached ring carbon atom (ρ_C) by the McConnell relation (McConnell, 1956):

$$A_{iso} = Q\rho_C$$

where A_{iso} is the isotropic hyperfine coupling constant [i.e., $^1/_3(A_{||} + 2A_{\perp})$] and Q is a constant equal to 106 MHz. The spin density at C(2) of A_1 is therefore 0.096 compared to 0.073 in $PhQ^{\bullet-}$. While this difference is only 0.023 of an electron in absolute terms, it represents an increase of 31% relative to $PhQ^{\bullet-}$. Changes in the spin density at C(3) are also suggested by the changes in the 1′-methylene hfc. However, the dependence of the hfcs on the orientation of the methylene group relative to the plane of the quinone ring (Heller & McConnell, 1960) makes such differences in spin density impossible to quantitate. Clearly, the protein environment of A_1 causes a change in the unpaired electron spin density distribution within $A_1^{\bullet-}$ relative to $PhQ^{\bullet-}$. Such a change in the electronic structure of A_1 could be responsible for the its low E_m through destabilization of the SOMO which contains the transferred electron. It should be noted that the methyl A_{iso}'s of $PhQ^{\bullet-}$ and $2MNQ^{\bullet-}$ differ by only 0.2 MHz. This small difference suggests that the nature and conformation of the substituent at C(3) have little effect on the electron spin density distribution, and therefore protein induced differences in the conformation of the phytyl side chain of A_1 are not responsible for its unusual spin density distribution.

The H-bond hfcs are dependent on both the unpaired electron spin density at the oxygen atom (ρ_O) and the O−H distance (r) according to the equation (Feher et al., 1988):

$$A_{\perp}, A_{||} \propto \rho_O(1/r^3)$$

Thus the differences between the H-bond hfcs of $A_1^{\bullet-}$ and $PhQ^{\bullet-}$ could arise due to ρ_O being *ca*. 2 times larger for $A_1^{\bullet-}$ than for $PhQ^{\bullet-}$, or if the O−H distance (r) in $A_1^{\bullet-}$ is *ca*. 0.8 times that in $PhQ^{\bullet-}$. These two effects are not mutually exclusive, since changes in O−H distance affect the polarization of the C−O bond and hence the spin density at the oxygen, and the real situation probably involves differences in spin density and distance. Support for a difference in the spin densities at O is provided by the EPR spectra. The shoulder on the low-field side of the $A_1^{\bullet-}$ EPR spectrum is suggestive of an increase in g_x, the lowest field g value of semiquinone anion radicals. Such an increase can arise from an increase in ρ_O (Stone, 1963; Burghaus et al., 1993). However, other factors can also influence the magnitude of g_x (Stone, 1963; Burghaus et al., 1993). A decrease in the energy of the antibonding π orbital (π* orbital), such as can arise from aromatic $\pi-\pi$ stacking interactions, or an increase in the energy of the nonbonding orbital, which can be brought about in quinones by weakening the hydrogen bonding, can also increase g_x. A similar increase in g_x for $A_1^{\bullet-}$ has been suggested from K-band EPR of the $P700^{\bullet+}-A_1^{\bullet-}$ spin polarized state (van der Est et al., 1995), although those authors preferred to interpret this as arising from a weakening of the H-bonding. Recent ENDOR studies using ^{13}C labeled ubiquinone-10 and ubiquinone-0 (Samoilova et al., 1994, 1995) have shown that hydrogen bonding to both quinone carbonyls of the ubisemiquinone anion radical leads to increased spin density at C(3) and C(2) (C(2) and C(3) respectively in phylloquinone) and hence an increase in the methyl group and β-CH_2 ^1H hfcs as we observe here. It is possible that both H-bond hfcs arise from protons hydrogen bonded to the same quinone oxygen, but such a situation has not been reported in previous ENDOR studies of semiquinone radicals *in vivo* or *in vitro* (Lubitz et al., 1985; MacMillan et al., 1995; Rigby et al., 1995).

The results presented here show that protein−quinone interactions at the A_1 binding site of PS1 alter the unpaired electron spin density distribution within the reduced radical state $A_1^{\bullet-}$. More electron spin is located at C(2), and also possibly at C(3), in $A_1^{\bullet-}$ than in $PhQ^{\bullet-}$. The hydrogen bond O−H distances are shorter and/or the spin density at the oxygens is greater in $A_1^{\bullet-}$ than in $PhQ^{\bullet-}$. Further studies are required to determine which of these effects is responsible for the unusual E_m of A_1.

REFERENCES

Barry, B. A., & Babcock, G. T. (1987) *Proc. Natl. Acad. Sci. U.S.A. 84*, 7099.

Barry, B. A., Bender, C. J., McIntosh, L., Ferguson-Miller, S., & Babcock, G. T. (1988) *Isr. J. Chem. 28*, 129.

Biggins, J., & Mathis, P. (1988) *Biochemistry 27*, 1494.

Burghaus, O., Plato, M., Rohrer, M., Möbius, K., MacMillan, F., & Lubitz, W. (1993) *J. Phys. Chem. 97*, 7639.

Currier, T. C., Haury, J. F., & Wolk, C. P. (1977) *J. Bacteriol. 129*, 1556.

Deisenhofer, J., & Norris, J. R., Eds. (1993) *The Photosynthetic Reaction Centre*, Vols. 1 and 2, Academic Press, San Diego, CA.

Dinse, K. P., Biehl, R., & Möbius, K. (1974) *J. Chem. Phys. 61*, 4335.

Dorio, M. M., & Freed, J. H., Eds. (1979) *Multiple Electron Resonance Spectroscopy*, Plenum Press, New York.

Evans, M. C. W., & Nugent, J. H. A. (1993) in *The Photosynthetic Reaction Centre* (Deisenhofer, J., & Norris, J. R., Eds.) Vol. 1, p 391, Academic Press, San Diego, CA.

Feher, G., Isaacson, R. A., Okamura, M. Y., & Lubitz, W. (1988) in *The Photosynthetic Bacterial Reaction Centre: Structure and Dynamics* (Breton, J., & Vermeglio, A., Eds.) pp 229−235, Plenum Press, New York.

Freed, J. H. (1969) *J. Chem. Phys. 50*, 2271.

Golbeck, J. H. (1992) *Annu. Rev. Plant Physiol. Plant Mol. Biol. 43*, 293.

Hales, B. J., & Case, E. E. (1981) *Biochim. Biophys. Acta 637*, 291.

Heathcote, P., Hanley, J. A., & Evans, M. C. W. (1993) *Biochim. Biophys. Acta 1144*, 54.
Heathcote, P., Moënne-Loccoz, P., Rigby, S. E. J., & Evans, M. C. W. (1996) *Biochemistry 35*, 6644.
Heller, H. C., & McConnell, H. M. (1960) *J. Chem. Phys. 32*, 1535.
Hoganson, C. W., & Babcock, G. T. (1992) *Biochemistry 31*, 11874.
Itoh, S., Iwaki, M., & Ikegami, I. (1987) *Biochim. Biophys. Acta 898*, 508.
Kurreck, H., Kirste, B., & Lubitz, W. (1988) *Electron Nuclear Double Resonance Spectroscopy of Radicals in Solution; Application to Organic and Biological Chemistry*, VCH Publishers, Weinheim, Germany.
Lubitz, W., Abresch, E. C., Debus, R. J., Isaacson, R. A., Okamura, M. Y., & Feher, G. (1985) *Biochim. Biophys. Acta 808*, 464.
MacMillan, F., Lendzian, F., Renger, G., & Lubitz, W. (1995) *Biochemistry 34*, 8144.
Mansfield, R. W., & Evans, M. C. W. (1988) *Isr. J. Chem. 28*, 97.
Mansfield, R. W., Hubbard, J. A. M., Nugent, J. H. A., & Evans, M. C. W. (1987) *FEBS Lett. 220*, 74.
McConnell, H. M. (1956) *J. Chem. Phys. 24*, 764.
Muto, H., & Iwasaki, M. J. (1973) *J. Chem. Phys. 59*, 4821.
O'Malley, P. J., & Babcock, G. T. (1984) *J. Chem. Phys. 80*, 3912.
O'Malley, P. J., & Babcock, G. T. (1986) *J. Am. Chem. Soc. 108*, 3995.
Palace, G. P., Franke, J. E., & Warden, J. T. (1987) *FEBS Lett. 215*, 58.
Rigby, S. E. J., Nugent, J. H. A., & O'Malley, P. J. (1994a) *Biochemistry 33*, 1734.
Rigby, S. E. J., Nugent, J. H. A., & O'Malley, P. J. (1994b) *Biochemistry 33*, 10043.
Rigby, S. E. J., Heathcote, P., Evans, M. C. W., & Nugent, J. H. A. (1995) *Biochemistry 34*, 12075.
Rustandi, R. R., Snyder, S. W., Feezel, L. L., Michalski, T. J., Norris, J. R., Thurnauer, M. C., & Biggins, J. (1990) *Biochemistry 29*, 8030.
Samoilova, R. I., van Liemt, W. B. S., Steggerda, W. F., Lugdenberg, J., Hoff, A. J., Spoyalov, A. P., Tyryshkin, N. P., Gritzan, N. P., & Tsvetkov, Yu. D. (1994) *J. Chem. Soc., Perkin Trans. 2*, 609.
Samoilova, R. I., Gritzan, N. P., Hoff, A. J., van Liemt, W. B. S., Lugdenberg, J., Spoyalov, A. P., & Tsvetkov, Yu. D. (1995) *J. Chem. Soc., Perkin Trans. 2*, 2063.
Sétif, P., & Bottin, H. (1989) *Biochemistry 28*, 2689.
Sétif, P., & Bottin, H. (1991) *Biochim. Biophys. Acta 1057*, 331.
Snyder, S. S., Rustandi, R. R., Biggins, J., Norris, J. R., & Thurnauer, M. C. (1991) *Proc. Natl. Acad. Sci. U.S.A. 88*, 9895.
Stone, A. J. (1963) *Mol. Phys. 6*, 509.
van der Est, A., Sieckmann, Lubitz, W., & Stehlik, D. (1995) *Chem. Phys. 194*, 349.
Ziegler, K., Lockau, W., & Nitschke, W. (1987) *FEBS Lett. 217*, 16.

BI952619X